Geomechanics and Engineering, *Vol. 7, No. 3 (2014) 233-246*
DOI: http://dx.doi.org/10.12989/gae.2014.7.3.233

A new geomechanical approach to investigate the role of in-situ stresses and pore pressure on hydraulic fracture pressure profile in vertical and horizontal oil wells

Seyed Erfan Saberhosseini *[1], Reza Keshavarzi [2] and Kaveh Ahangari [3]

[1] *Department of Petroleum Engineering, Science and research branch, Islamic Azad University, Tehran, Iran*
[2] *Young Researchers and Elites Club, Science and Research Branch, Islamic Azad University, Tehran, Iran*
[3] *Department of Mining Engineering, Science and Research Branch, Islamic Azad University, Tehran, Iran*

(*Received October 09, 2013, Revised May 03, 2014, Accepted May 10, 2014*)

Abstract. Estimation of fracture initiation pressure is one of the most difficult technical challenges in hydraulic fracturing treatment of vertical or horizontal oil wells. In this study, the influence of in-situ stresses and pore pressure values on fracture initiation pressure and its profile in vertical and horizontal oil wells in a normal stress regime have been investigated. Cohesive elements with traction-separation law (XFEM-based cohesive law) are used for simulating the fracturing process in a fluid-solid coupling finite element model. The maximum nominal stress criterion is selected for initiation of damage in the cohesive elements. The stress intensity factors are verified for both XFEM-based cohesive law and analytical solution to show the validation of the cohesive law in fracture modeling where the compared results are in a very good agreement with less than 1% error. The results showed that, generally by increasing the difference between the maximum and minimum horizontal stress, the fracture pressure and its profile has been strongly changed in the vertical wells. Also, it's been clearly observed that in a horizontal well drilled in the direction of minimum horizontal stress, the values of fracture pressure have been significantly affected by the difference between overburden pressure and maximum horizontal stress. Additionally, increasing pore pressure from under-pressure regime to over-pressure state has made a considerable fall on fracture pressure in both vertical and horizontal oil wells.

Keywords: hydraulic fracturing; in-situ stress; pore pressure; fracture pressure profile; cohesive elements; finite element; XFEM-based cohesive law

1. Introduction

Two of the most important parameters which have significant effects on fracture pressure initiation are in-situ stresses and the pore pressure condition which is illustrated by under-pressure, normal and over-pressure states (Fjaer 2008, Valco and Economides 1997). According to the fracture mechanics and reservoir engineering literature, in-situ stresses and pore pressure act

*Corresponding author, M.Sc., E-mail: erfansaberhosseini@gmail.com

http://www.techno-press.org/?journal=gae&subpage=7 ISSN: 2005-307X (Print), 2092-6219 (Online)

inversely to each other which mean that for example increasing minimum horizontal stress or decreasing pore pressure causes massive rise on fracture initiation pressure (Fjaer 2008). Also, from the geological point of view, tectonic forces which are originated from underground geological activities strongly influence the hydraulic fracture initiation pressure in horizontal and vertical oil wells by changing in-situ stresses such as vertical and horizontal stresses or pore pressure regimes (Fjaer 2008). The in-situ stress and pore pressure changes are initiated from those geological actions and have great effects on fracture initiation pressure (Valco and Economides 1997). Therefore, a numerical study of in-situ stress or pore pressure effects on fracture initiation pressure can be so beneficial for geological and reservoir studies in oil and gas fields.

The cohesive elements method has its origin in the concepts of a cohesive zone model for fractures which originally proposed by Dugdale (1960) and Barenblatt (1962) are used to simulate the fracture initiation in the ABAQUS program. The finite element method is applied for constructing the surrounding materials and the cohesive elements with XFEM-based traction separation law (cohesive law) are used for fracture initiation into the model. The cohesive elements damage calculations are based on XFEM-based traction-separation law (ABAQUS 2011).

Among many studies which were conducted in the past in hydraulic fracturing area and the use of cohesive elements for designing the fracturing process, there is a research gap regarding the effect of pore pressure and in-situ stress condition on hydraulic fracture initiation pressure which is a very important technical challenging parameter in oil and gas reservoirs stimulation. Nonetheless, many authors have worked on various cases of hydraulic fracturing; Sarris and Papanastasiou (2011), have investigated the influence of cohesive process zone in hydraulic fracture modeling; Chen *et al*. (2011) have applied the cohesive element method to model a viscosity dominated hydraulic fracture; Zhang *et al*. (2010) have worked on three-dimensional finite element simulation of hydraulic fracture for horizontal well; Chen *et al*. (2009) have focused on cohesive zone finite element based modeling of hydraulic fractures; Settari and Cleary (1984) worked on three-dimensional simulation of hydraulic fracturing; Zhu *et al*. (2014) have studied on hydraulic fracturing experiments of highly deviated well with oriented perforation technique; but the lack of details in study of in-situ stress and pore pressure changes on fracture initiation pressure is still sensed. In our study the focus would be on the influential in-situ stresses and pore pressure regimes which are affecting the fracture pressure and its profile. Since our study is performed in a normal stress regime, this means that in our investigation in vertical wells (which is drilled in the direction of overburden pressure) the difference between maximum and minimum horizontal stress is considered and for example in a horizontal well drilled in the direction of minimum horizontal stress, the difference between overburden pressure and maximum horizontal stress is taken into account. Therefore a new geo-mechanical approach based on numerical modeling is considered in vertical and horizontal oil wells in three depths with the normal fault regime assumption for investigating the effect of in-situ stress conditions and pore pressure regimes on fracture initiation pressure and its profile.

2. Traction-separation law

The traction-separation or cohesive law defines the relationship between the traction tensor t and the displacement jump δ across a pair of cohesive surfaces (Tomar *et al*. 2004). A cohesive potential function φ is defined so that the traction is given by

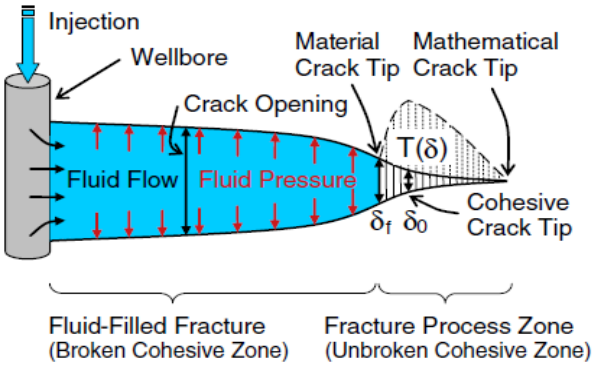

Fig. 1 Schematic view of fracture and fluid flow

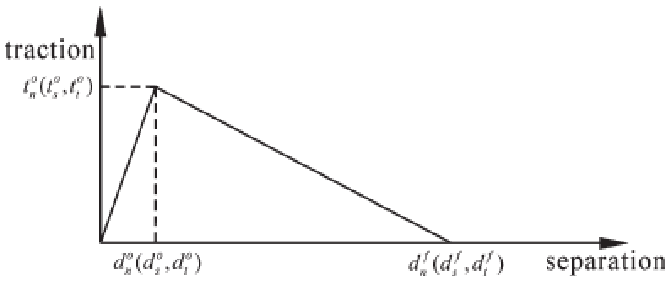

Fig. 2 Typical traction-separation law

$$t = \frac{\partial \varphi}{\partial \delta} \tag{1}$$

This law assumes that the cohesive surfaces are intact without any relative displacement, and exhibit linear elastic behavior until the traction reaches the cohesive strength $T_{\max}$ (Tensile strength) or equivalently the separation exceeds δ_0 (Initial displacement at initiation of fracture). Beyond δ_0, the traction reduces linearly to zero up to δ_f (Final displacement at complete failure) and any unloading takes place irreversibly (Chen 2011) as shown in Fig. 1.

The mechanical constitutive behavior of the cohesive elements can be defined by using a constitutive model specified directly in terms of traction versus separation. When pore pressure cohesive elements are used in soils procedures in ABAQUS, the fluid constitutive behavior of the cohesive elements can be defined by considering the tangential fluid flow relationship, and by defining fluid leak-off coefficients (ABAQUS 2011).

2.1 Damage initiation

Damage initiation refers to the beginning of degradation of the response of a material point. The process of degradation begins when the stresses satisfy certain damage initiation criteria and after this point the non-linear behavior of the traction-separation will be started as damage developed (Camanho and Davila 2002, Zhang *et al*. 2010). According to Fig. 2, t_n^0, t_s^0 and t_t^0 represent the peak values of the nominal stresses; d_n^0, d_s^0 and d_t^0 are the displacement peak values at initiation of damage and d_n^f, d_s^f and d_t^f are the displacement peak values at complete failure in the normal and shear directions.

2.2 Maximum nominal stress criterion

Damage is assumed to initiates when the maximum nominal stress ratio (as defined in the expression below) reaches a value of one. The symbol <> signifies that a pure compressive deformation or stress state does not initiate damage (Zhang *et al*. 2010, ABAQUS 2011). Figs. 3 and 4, show the peak values of fracture initiation pressure (kPa) at the depth of 2175 m for both vertical and horizontal wells which their values are presented in Table 5 and 6. Several damage initiation criteria are available but the maximum nominal stress criterion (MAXS) is considered because of its convenience and efficiency. A value of 1 or higher indicates that the initiation criterion has been met. This criterion can be represented as

$$\mathrm{Max}\left\{\frac{< t_n >}{t_n^0}, \frac{t_s}{t_s^0}, \frac{t_t}{t_t^0}\right\} = 1 \tag{2}$$

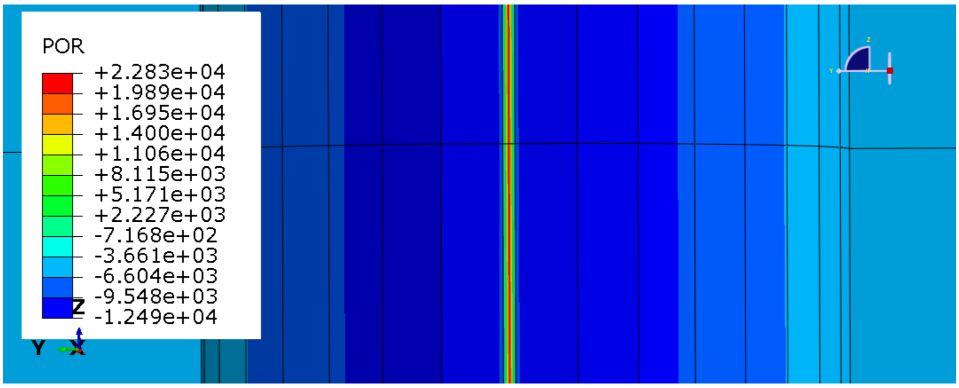

Fig. 3 Fracture initiation pressure contours in the vertical well (at the depth of 2175 m)

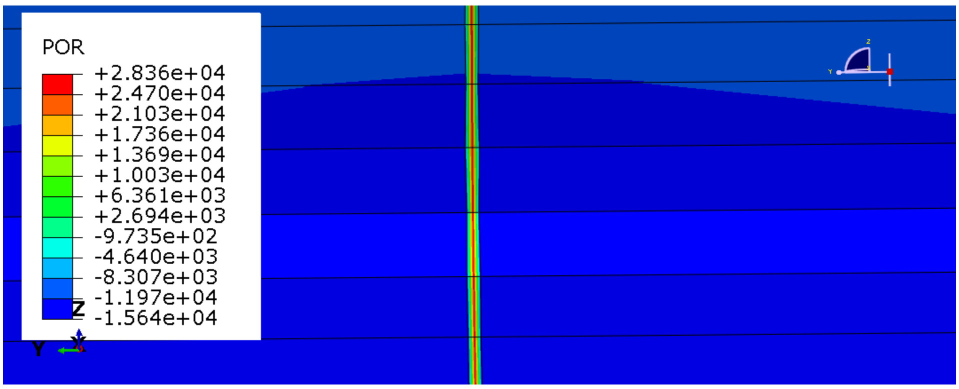

Fig. 4 Fracture initiation pressure contours in the horizontal well (at the depth of 2175 m)

3. Fluid flow into the fracture

3.1 Tangential flow into the fracture

The fluid flow model in the fracture consists of tangential and normal flow (Fig. 5). The term of tangential flow of fluid is referred as the flowing of fluid just into the fracture gap (Chen 2011). To allow tangential flow, gap flow property has to be defined in conjunction with the pore fluid material definition. The fluid is assumed to be incompressible with Newtonian rheology.

3.2 Newtonian rheology

Tangential flow within the gap is governed by the lubrication equations (Batchelor 1967), which is formulated from Poiseulle's law.

$$q = \frac{-\left(k_t \times \nabla . p_f\right)}{w} \tag{3}$$

Where the q is flow rate of tangential flow into the gap; K_t is the tangential permeability that is defined below; $\nabla.P_f$ is the fluid pressure gradient along the cohesive zone and w is the gap (fracture) opening and the K_t is defined in the following equation.

$$k_t = \frac{w^3}{12\mu} \tag{4}$$

μ is the fluid viscosity.

3.3 Normal fluid flow into the fracture

The normal flow is defined as a flow of fluid from rock matrix into the fracture gap due to pressure difference between the formation pore pressure and the fracture gap (Fig. 5). Normal flow can be defined as fluid leak-off properties in ABAQUS which contains top and bottom constant coefficients (Valco and Economides 1997). The normal flow or the rate of normal flow at the top and bottom of the cohesive elements are defined as follows

$$q_t = c_t\left(p_f - p_t\right) \tag{5}$$

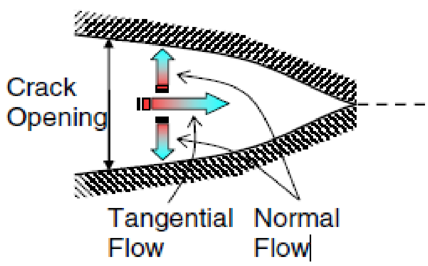

Fig. 5 Schematic view of tangential and normal fluid flow into the fracture

$$q_b = c_b\left(p_f - p_b\right) \tag{6}$$

Where Q_t and Q_b are the top and bottom flow rate respectively; P_f is cohesive element middle pressure. The terms P_t and P_b *a*re top and bottom pressure of the cohesive elements respectively; C_t and C_b are the top and bottom leak-off coefficients.

3.4 Governing equation of fracture fluid flow

The continuity equation of mass conservation which is presented below is the governing equation of fluid flow into the fracture and the adjacent porous material (Peirce and Detournay 2008). The continuity equation of mass conservation is

$$\frac{\partial w}{\partial t} + \nabla . q + \left(q_t + q_b\right) = Q(t).\,\delta(x, y) \tag{7}$$

Where q is the fluid flux of the tangential flow; w is the crack opening; $Q(t)$ is the injection rate; q_t and q_b are the normal flow rates into the top and bottom surfaces of the cohesive elements respectively which reflect the leak-off through the fracture surfaces into the adjacent material.

By combining Eqs. (3), (4) and (7), the extracted Reynolds lubrication equation (Eq. (8)) can show the fluid conjunction and continuity between adjacent porous medium fluid and the fracture fluid flow.

$$\frac{\partial w}{\partial t} + c_t\left(p_f + p_t\right) + c_b\left(p_f - p_t\right) = \frac{1}{12\mu}\nabla.\left(w^3 \nabla . p_f\right) + Q(t).\,\delta(x, y) \tag{8}$$

4. Numerical results

4.1 Single-edged notch specimen verification

Stress Intensity Factor (SIF) is widely used in fracture mechanics; and its accurate estimation for postulated flaws under given load conditions is an important aspect of the use of fracture mechanics (Tada *et al*. 1973, ABAQUS 2011). To verify the capability of XFEM-based traction-separation law for modeling fracture used in this study, a linear elastic plane strain single-edged notch specimen under mode I loading, is considered as shown in Fig. 6, which Bowie (1964) has provided a series solution for the stress intensity factor. For the plane strain case, a three-dimensional model is used (Fig. 7) with one layer of elements in the thickness direction to verify the fracturing process (XFEM-based traction-separation law) and the capability for evaluating the SIF. The specimen is loaded in Mode I by uniform tension force applied to its top and bottom surfaces. The symmetry about $x = 0$ can be used to model only half of the plate.

Fig. 8 shows the fracture initiation of the XFEM-based cohesive approach model and the Mises stress contours within the enriched or cohesive area. When the extended finite element method is used, the mesh is not required to match the cracked geometry. The presence of a crack is ensured by the special enriched functions in conjunction with additional degrees of freedom. This approach also removes the requirement to explicitly define the crack front or to specify the virtual crack extension direction when evaluating the contour integral such as stress intensity factor (Huang *et al*. 2003). The XFEM-based crack results obtained by ABAQUS program and the results gained by analytical solution (Huang *et al*. 2003) for the stress intensity factor $\left(\sigma\sqrt{\pi a}\right)$ are in a very good agreement with less than one percent error.

This verification implies that the XFEM-based cohesive law is strongly consistent with analytical results. The comparison between XFEM-based, analytical and normalized SIF (XFEM SIF/analytical SIF) versus tension forces for the single-edged crack model are presented in Table 1.

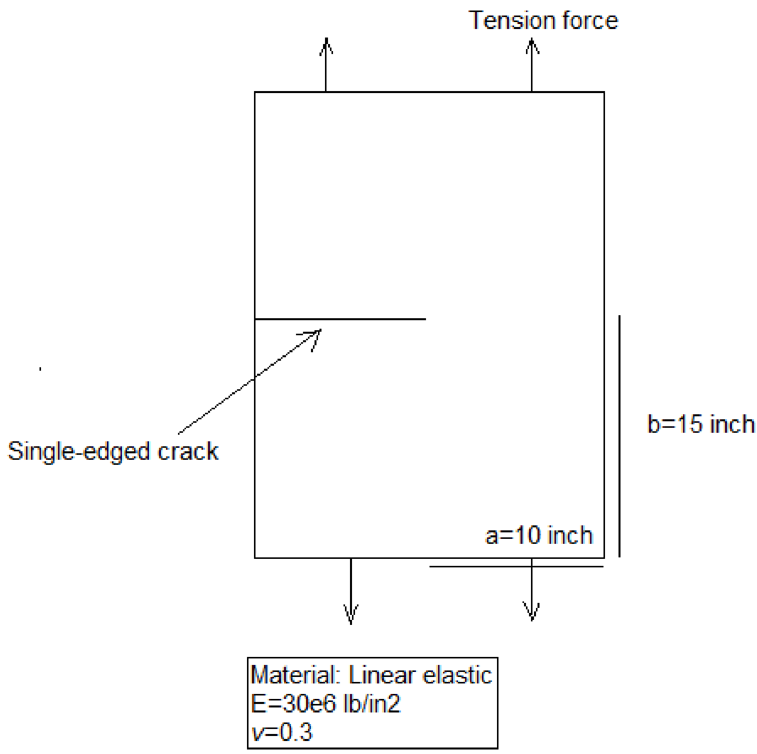

Fig. 6 Analytical single-edged crack

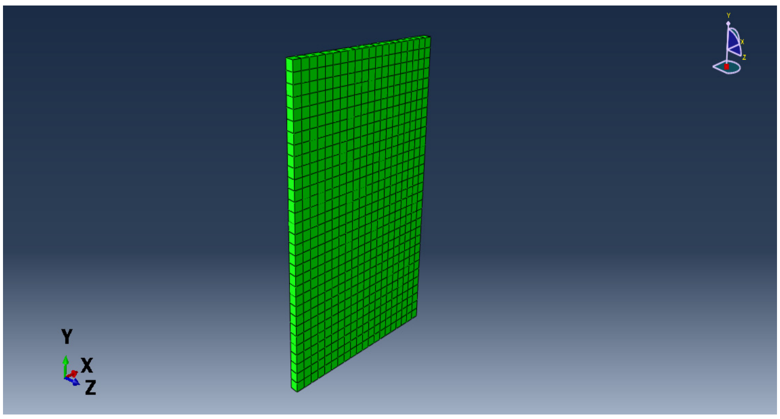

Fig. 7 XFEM meshed crack model

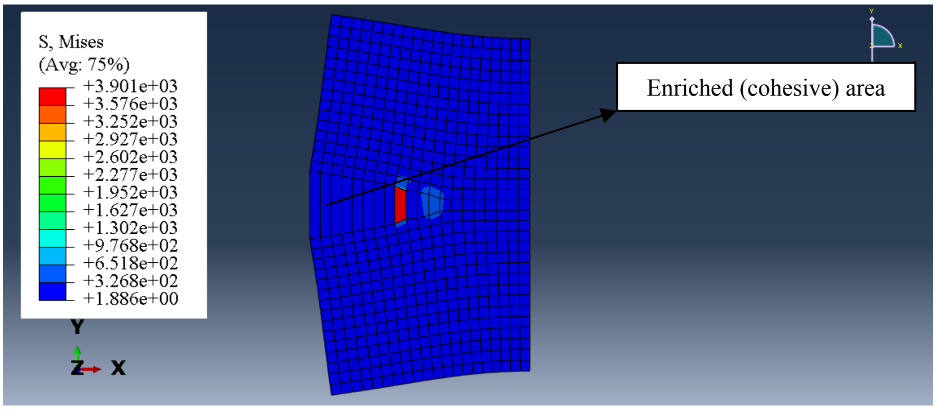

Fig. 8 XFEM-based cohesive modeling of a single-edged crack after fracture initiation

Table 1 XFEM, analytical and Normalized SIF versus tension forces for the single-edged notch crack problem

Tension force (lb/in^2)	SIF analytical $(\sigma\sqrt{\pi a})$ SIF XFEM	Normalized SIF $\left(\frac{K_I}{(\sigma\sqrt{\pi a})}\right)$
100	560.35	0.994251
150	840.53	0.994246
200	1120.71	0.994244
250	1400.89	0.994239
300	16.81.07	0.994241
350	1961.24	0.994243
400	2241.42	0.994244
450	2521.6	0.994241
500	2801.78	0.994242
550	3081.96	0.994240
600	3365.14	0.994241

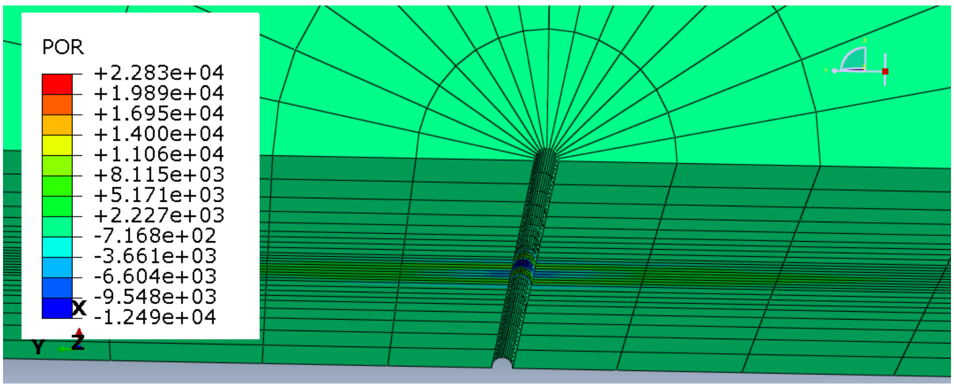

Fig. 9 The 3D view of vertical well hydraulic fracture model (at the depth of 2175 m)

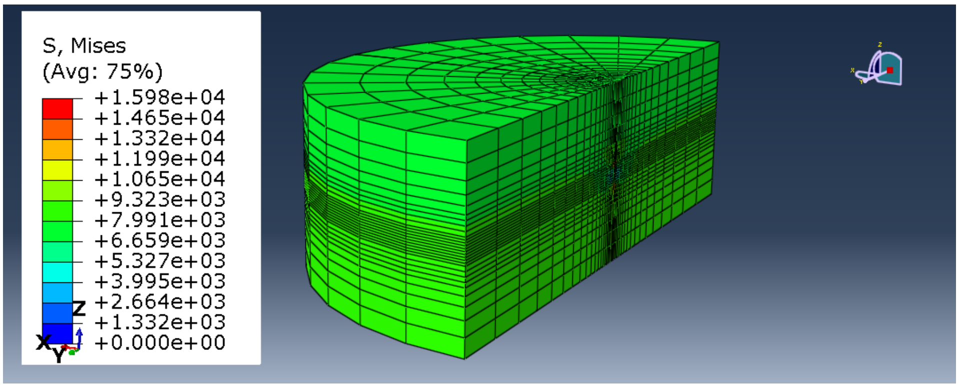

Fig. 9 Continued

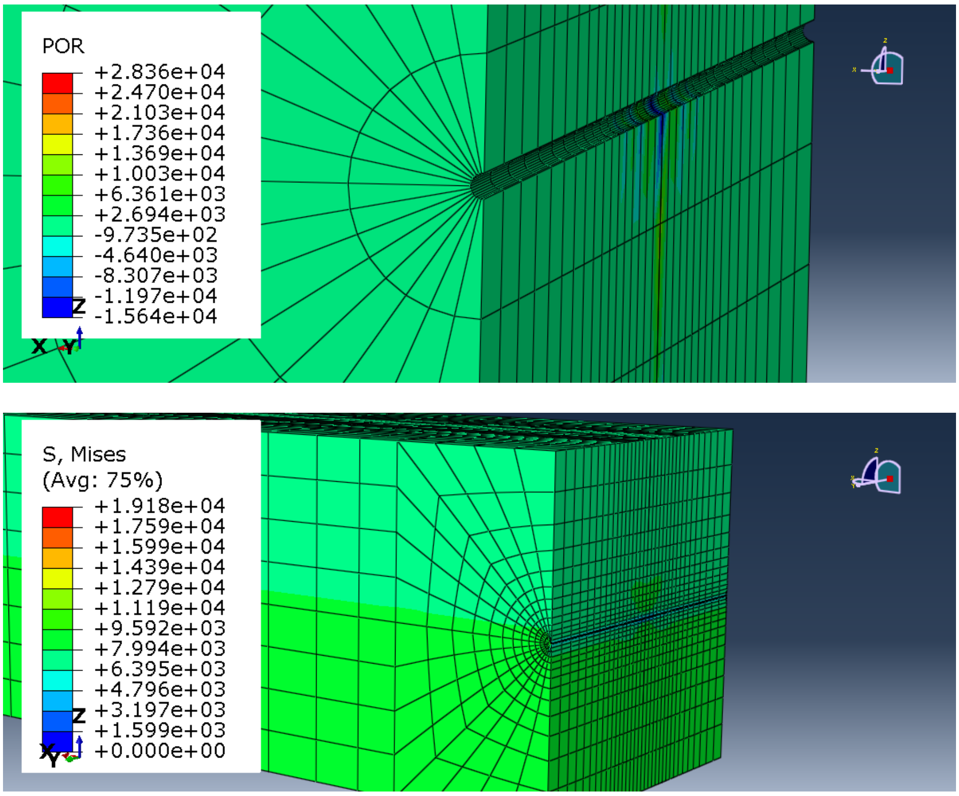

Fig. 10 The 3D view of horizontal well hydraulic fracture model (at the depth of 2175 m)

4.2 Reservoir hydraulic fracture model and its material

In this study, the reservoir top depths for both horizontal and vertical wells model are in the depths of 2100 m, 2600 m and 3100 m from surface. Whole reservoir area is considered as a large semicircular with the radius of 250 m and the height of 150 m for vertical well model (Fig. 9) and

Table 2 Formation materials

Void ratio	Elastic module (GPa)	Permeability (md)
0.2	40	1

Table 3 Cohesive zone materials

t_n (MPa)	t_s (MPa)	t_t (MPa)	d_n^f (m)	Gap flow viscosity (Pa.s)
6	*2*	*2*	0.005	10^{-3}

a semi-rectangular is considered with 250 m length, 100 m width and 150 m height for the horizontal well model (Fig. 10). Both horizontal and vertical well hydraulic fracture models are symmetric about *Y-Z* plane.

The fracturing operation started with the flow rate of 10 bbl/min which has been accomplished after 20 minutes injection of fracturing fluid. There are two basic materials in the models; the cohesive zone material and formation material (adjacent porous medium). Cohesive zone material is located in the middle of the model and is tied to the sides of the formation rocks. The formation and cohesive zone materials are defined for both horizontal and vertical wells model in Tables 2 and 3.

4.3 The influence of in-situ stress on fracture initiation pressure

The in-situ stresses in each depth are presented in Table 4 with default K_{max} = 0.9 and K_{min} = 0.8 where K_{max} is the ratio of maximum horizontal stress to vertical stress; K_{min} is the ratio of minimum horizontal stress to vertical stress. For investigating the effect of in-situ stress on fracture initiation pressure in vertical well, the focus would be on $\Delta\sigma_h$ (the difference between maximum and minimum horizontal stress) and overburden pressure was assumed to be constant and different values of $\Delta\sigma_h$ and K_{min} were considered as shown in Table 5. The results show that, any decrease in $\Delta\sigma_h$ leads to increasing the fracture initiation pressure (Table 5). Based on Table 5, the values of fracture initiation pressure in the three depths of 2175 m, 2675 m and 3175 m have been considerably affected by $\Delta\sigma_h$ values. In other words, for example at the depth of 2175 m when $\Delta\sigma_h$ has changed from 13.05 MPa to 8.7 MPa the value of fracture initiation pressure has increased from 22.83 MPa to 33.56 MPa or at the depth of 3175 m as $\Delta\sigma_h$ has decreased from 19.05 MPa to 6.35 MPa the value of fracture initiation pressure has increased from 30.71 MPa to 67.92 MPa. Also, to analyze the role of in-situ stress conditions in horizontal wells drilled in the direction of minimum horizontal stress, $\Delta\sigma_v$ (the difference between overburden pressure and maximum horizontal stress as well as K_{max} have been taken into account (Table 6). The results

Table 4 Default values of in-situ stresses and pore pressure in three various depths

Depth (m)	σ_v (MPa)	σ_H (MPa)	σ_h (MPa)	Pore pressure (MPa)
2175	43.5	39.15	30.45	21.31
2675	53.5	48.15	37.45	26.21
3175	63.5	57.15	44.45	31.11

Table 5 The effect of $\Delta\sigma_h$ (σ_H-σ_h) on fracture initiation pressure (P_f) in a vertical well

Depth (m)	σ_h (MPa)	$\Delta\sigma_h$ (MPa)	$K_{\min}$	$K_{\max}$	P_f (MPa)
2175	26.1	13.05	0.6	0.9	22.83
	30.45	8.7	0.7	0.9	33.56
	34.8	4.35	0.8	0.9	43.09
2675	32.1	16.05	0.6	0.9	27.71
	37.45	10.7	0.7	0.9	41.3
	42.8	5.35	0.8	0.9	55
3175	38.1	19.05	0.6	0.9	30.71
	44.45	12.7	0.7	0.9	43.52
	50.8	6.35	0.8	0.9	67.92

Table 6 The effect of $\Delta\sigma_v$ (σ_v-σ_H) on fracture initiation pressure (P_f) in a horizontal well

Depth (m)	σ_H (MPa)	$\Delta\sigma_v$ (MPa)	$K_{\min}$	$K_{\max}$	P_f (MPa)
2175	30.45	13.05	0.6	0.7	28.36
	34.8	8.7	0.6	0.8	40
	39.15	4.35	0.6	0.9	51
2675	37.45	16.05	0.6	0.7	37.8
	42.8	10.7	0.6	0.8	55.4
	48.15	5.35	0.6	0.9	72.77
3175	44.45	19.05	0.6	0.7	42.14
	50.8	12.7	0.6	0.8	62.53
	57.15	6.35	0.6	0.9	75.34

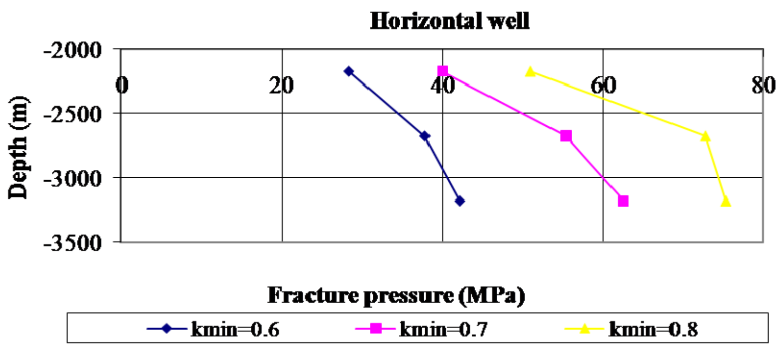

Fig. 11 The effect of $\Delta\sigma_v$ (σ_v-σ_H) on fracture pressure profile in the horizontal well

imply that increasing $\Delta\sigma_v$ would lead to decreasing the value of fracture initiation pressure. For instance, at the depth of 2175 m when $\Delta\sigma_v$ has decreased from 13.05 MPa to 4.35 MPa the value of fracture initiation pressure has increased from 28.36 MPa to 51 MPa or at the depth of 3175 m as $\Delta\sigma_v$ has changed from 19.05 MPa to 6.35 MPa the value of fracture initiation pressure has

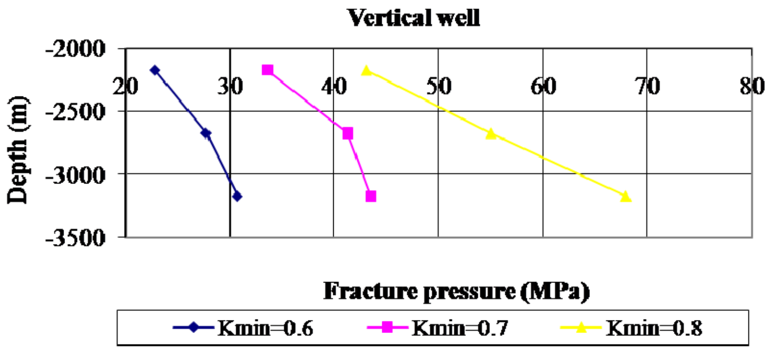

Fig. 12 The effect of $\Delta\sigma_h$ (σ_H-σ_h) on fracture pressure profile in the vertical well

increased from 42.14 MPa to 75.34 MPa. Also, the effect of in-situ stress on fracture initiation pressure is represented in Figs. 11 and 12.

4.4 The Influence of pore pressure on fracture initiation pressure

In this section, three values of pore pressure have been assumed from under pressure to over pressure regime in the three different depths with K_{max} = 0.9 and K_{min} = 0.8 as the constant values for in-situ horizontal stresses. The hydrostatic pore pressure with 10 kN/m^{3}and 9.8 kN/m^3 as water and oil specific gravity are considered as the normal pore pressure regime for each depth. The results showed that, by increasing pore pressure from under pressure to over pressure state, the fracture pressure is influenced severely for both vertical and horizontal wells as shown in Table 7. According to the results, increasing pore pressure from under-pressure to over-pressure regime, caused a considerable fall on fracture initiation pressure and its profile in both vertical and horizontal wells. For instance, at the depth of 2675 m when pore pressure value has increased from 16.735 MPa to 36.735 MPa the value of fracture initiation pressure for vertical well has been decreased from 63.33 MPa to 43 MPa while for the horizontal well this value has been decreased

Table 7 The effect of pore pressure on fracture initiation pressure (P_f) in both vertical and horizontal wells

Depth (m)	Pore pressure (MPa)	Fracture pressure in a vertical well (MPa)	Fracture pressure in a horizontal well (MPa)
2175	11.735	57.75	68.34
	21.735	43.09	52.79
	31.735	35	49.38
2675	16.735	63.33	72
	26.735	55	66.99
	36.735	43	51.08
3175	21.735	75	87.76
	31.735	67.92	80.89
	41.735	57	71.32

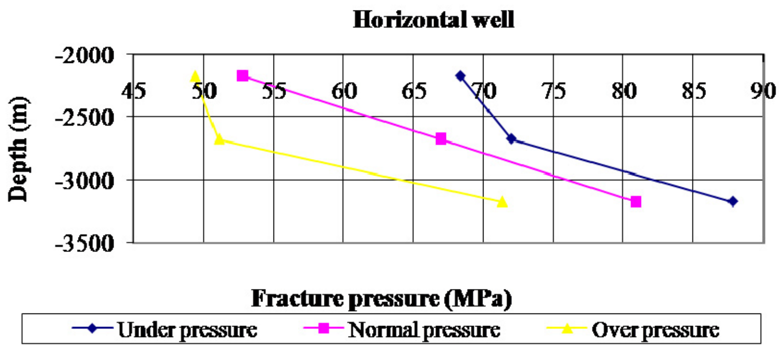

Fig. 13 Fracture pressure profiles for the horizontal well in different pore pressure regimes

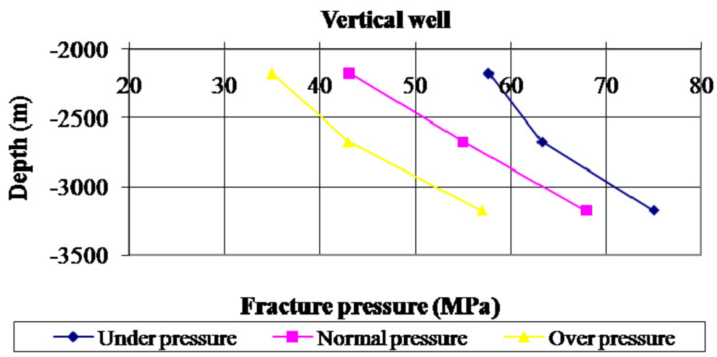

Fig. 14 Fracture pressure profiles for the vertical well in different pore pressure regimes

from 72 MPa to 51.08 MPa (Table 7). Also, the effect of pore pressure regime on fracture initiation pressure is represented in Figs. 13 and 14.

5. Conclusions

In this study, a numerical modeling approach has been proposed based on XFEM-based cohesive elements for modeling hydraulic fracture initiation problem in three-dimensional fluid-solid coupling model based on the ABAQUS software to account for the role of in-situ stress and pore pressure regimes on fracture initiation pressure in both vertical and horizontal oil wells. To verify the XFEM-based traction-separation law, a single-edged notch specimen was modeled; the SIF in both analytical and numerical models were compared to show the validation of the cohesive law. The compared results were in a very good agreement whereas the error was less than one percent. It’s been concluded that in-situ stress conditions would affect hydraulic fracture initiation pressure significantly in both vertical and horizontal wells whereas in vertical wells the difference between the maximum and minimum horizontal stress is the influential parameter while in horizontal wells drilled in the direction of minimum horizontal stress the difference between overburden pressure and maximum horizontal stress plays an important role on the value of fracture initiation pressure. Also, it's been clearly observed that the formation pore pressure regime would have considerable effects on hydraulic fracture initiation pressure. The pore pressure decline in various depths has increased the fracture pressure in both horizontal and vertical wells. The results from this study can be applied to explain the different values of fracture initiation pressure in various conditions of in-situ stress and pore pressure in both vertical and horizontal wells.

References

ABAQUS (2011), ABAQUS Documentation, Version 6. 11-1.

Barenblatt, G.I. (1962), "The mathematical theory of equilibrium of cracks in brittle fracture", *Advances in Applied Mechanics*, **7**, 55-129.

Batchelor, G.K. (1967), *An Introduction to Fluid Dynamics*, Cambridge University Press, London, UK, p. 615.

Bowie, O.L. (1964), "Rectangular tensile sheet with symmetric edge cracks", *Journal of Applied Mechanics*, **31**(2), 208-212.

Camanho, P.P. and Dávila, C.G. (2002), "Mixed-mode decohesion finite elements for the simulation of delamination in composite materials", NASA/TM-2002-211737, pp. 1-42.

Chen, Z. (2011), "Finite element modeling of viscosity-dominated hydraulic fractures", *Journal of Petroleum Science and Engineering*, **88-89**, 136-144.

Chen, Z.R., Bunger, A.P., Zhang, X. and Jeffrey, R.G. (2009), "Cohesive zone finite element based modeling of hydraulic fractures", *Acta Mech. Solida Sin.*, **22**(5), 443-452.

Dugdale, D.S. (1960), "Yielding of steel sheets containing slits", *Journal of the Mechanics and Physics of Solids*, **8**(2), 100-104.

Fjaer, E. (2008), *Petroleum Related Rock Mechanic*, Elsevier Publication Books, p. 491.

Huang, R., Sukumar, N. and Prevost, J.H. (2003), "Modeling quasi-static crack growth with the extended finite element method Part II: Numerical applications", *Int. J. Solids Struct.*, **40**, 7539-7552.

Peirce, A. and Detournay, E. (2008), "An implicit level set method for modeling hydraulically driven fractures", *Computer Methods in Applied Mechanics and Engineering*, **197**(33-40), 2858-2885.

Sarris, E. and Papanastasiou, P. (2011), "The influence of the cohesive process zone in hydraulic fracture modeling", *International Journal of Fracture*, **167**(1), 33-45.

Settari, A. and Cleary, M.P. (1984), "Three-dimensional simulation of hydraulic fracturing", *J. Pet. Technol.*, **36**(8), 1177-1190.

Tada, H., Paris, P.C. and Irwin, G.R. (1973), *The Stress Analysis of Cracks Handbook*, Del Research Corp., Hellertown, PA, USA.

Tomar, V., Zhai, J. and Zhou, M. (2004), "Bounds for element size in a variable stiffness cohesive finite element model", *Int. J. Numer. Method. Eng.*, **61**(11), 1894-1920.

Valco, P. and Economides, M.J. (1997), *Hydraulic Fracture Mechanics*, John Wiley & Sons Ltd., Texas A&M University, TX, USA.

Zhang, G.M., Liu, H., Zhang, J., Wu, H.A. and Wang, X.X. (2010), "Three-dimensional finite element simulation and parametric study for horizontal well hydraulic fracture", *Journal of Petroleum Science and Engineering*, **72**(3-4), 310-317.

Zhu, H.Y., Deng, J.G., Liu, S.J., Wen, M., Peng, C.Y., Li, J.R., Chen, Z.J., Hu, L.B., Lin, H. and Guang, D. (2014), "Hydraulic fracturing experiments of highly deviated well with oriented perforation technique", *Geomechanics and Engineering*, *Int. J.*, **6**(2), 153-172.

CC